JOURNAL OF CATALYSIS 45, 316–325 (1976)

The Characterization of CrO_x/SiO_2 Catalysts by Photoelectron Spectroscopy (XPS), X-Ray and Optical Measurements

A. CIMINO,[1] B. A. DE ANGELIS,[2] A. LUCHETTI,[2] AND G. MINELLI[1]

[1]*Centro di Studio sulla Struttura e Attività Catalitica di Sistemi di Ossidi del Consiglio Nazionale delle Ricerche (C.N.R.), Istituto di Chimica Generale e Inorganica, Università di Roma, Rome, Italy; and* [2]*Laboratori Ricerche di Base, Snamprogetti S.p.A., 00015 Monterotondo, Rome, Italy*

Received November 11, 1975

X-ray photoelectron spectroscopy (XPS or ESCA) has been applied, together with X-ray diffraction and diffuse reflectance spectroscopy, to the study of silica-supported CrO_3 in the concentration range 1 to 9 wt% Cr. The progressive reduction of Cr(VI) to Cr(III) caused by heat treatment has been followed. The stabilizing influence of the support on Cr(VI) at lower Cr contents is apparent. The X-ray diffraction pattern of the samples of higher Cr concentration reveals the presence of intermediate phases (Cr_8O_{23}, Cr_2O_5, CrO_2 for 9% Cr; CrO_2 for 5% Cr) which are known to occur in the decomposition of pure CrO_3. A drastic decrease of the intensity of the XPS $2p^{\frac{3}{2}}$ peak of Cr as a function of the temperature indicates an agglomeration of Cr_2O_3 into considerably large particles. The Cr(VI)/Cr(III) ratio as determined by XPS is larger than that obtained by chemical analysis. This discrepancy is explained by a model, valid for samples calcined at high temperature, in which a small part of Cr_2O_3 is present in a dispersed state (particles of diameter about equal to the probing depth of XPS) while the remaining part forms large particles of several hundred Å diameter.

INTRODUCTION

Supported chromia catalysts provide an example of the various problems encountered when dealing with an active component (chromia) dispersed over a so-called "inactive" support. Among the problems, one can quote the stabilization and the role of different valency states, the transformation of the initially added chromium component with temperature and/or outgassing treatments, the role played by the support as a mere disperser (thus acting only on the available surface area) as opposed to intrinsic chemical effects due to its interaction with the active oxide.

Studies aimed at elucidating these aspects have utilized several chemical and physical techniques. In view of their importance in practical applications, catalysts containing chromium oxides have received much attention, and much information is now available about their structure and their catalytic behavior (*1*, *2*). A large amount of the work reported in the literature is concerned with alumina or silica–alumina as supports, and a smaller part deals with CrO_x/SiO_2 (*3–9*). The interaction of chromium oxide with the support, as revealed by the stabilization of higher valence states, is lower on silica than on alumina or silica–alumina. It is, however, strong also on silica at low Cr concentrations (<1%).

An important problem is that concerning the state of aggregation of chromium. The formation of Cr_2O_3 crystallites, following different treatments, depends on the interaction with the support and affects to a large extent the performance of the catalyst.

Several techniques (thermogravimetric analysis, magnetic and optical measure-

ments, ESR spectroscopy) have been used on this system. X-ray photoelectron spectroscopy (XPS or ESCA) provides another useful tool since the information is coming from the external layers of the solid, on which attention is focused. It is interesting to see what information is coming out from this technique, compared to other techniques.

In the present paper we report the data obtained by XPS on silica-supported chromia, and we compare them with X-ray analysis and reflectance spectroscopy results obtained by us on the same samples.

EXPERIMENTAL

Specimen Preparation

The following commercial chemicals were used: CrO_3 (Alfa-Ventron), $(NH_4)_2$ Cr_2O_7 (Merck), Cr_2O_3 (Alfa-Ventron and Merck), K_2CrO_4, and $K_2Cr_2O_7$ (C. Erba).

Cr_2O_3 was prepared also by thermal decomposition of ammonium dichromate. $MgCr_2O_4$ was prepared by firing MgO and Cr_2O_3 at 1200°C for 50 hr. A single crystal of Cr_2O_3 and a sample of CrO_2 were obtained through the courtesy of M. Marezio and J. P. Remeika (Bell Laboratories).

Silica-supported samples were prepared by impregnation of Cabosil (Cabot Corp.), surface area 210 m^2/g, with a solution of CrO_3. The slurry was dried under careful and efficient agitation to avoid the formation of heterogencous samples, due to chromatographic effects; finally, it was left for 5 hr at 120°C. The following samples were prepared: CrSi 9 (8.99), CrSi 5 (4.90), CrSi 3 (2.92), CrSi 1 (0.99), where the figures in parentheses indicate the chromium content expressed as weight% of Cr.

Portions of these materials were heated for 5 hr, in air, at temperatures from 300 to 700°C. On several specimens surface area measurements (N_2, BET) were carried out after heat treatment; the values obtained were in the range 170–190 m^2/g.

The chemical analysis of Cr(VI) was based on the property that water removes CrO_3 from silica (*6*, *10*). Thus the analysis was carried out by contacting the samples with water for 36 hr, followed by centrifuging, adjustment to pH 2 with sulfuric acid, and absorbance measurement at 380 nm. Checks made by digesting the samples with dilute (0.1 *N*) sulfuric acid gave identical results.

Photoelectron Spectroscopy (XPS) Measurements

An AEI ES100 spectrometer, with Al (1486.6 eV) excitation was used. The powdered specimens were pressed into a trough, 1- to 2-mm deep and 6- × 15-mm^2 area, in a gold-plated metallic sample backing. Impurity carbon 1*s* line (283.8 eV) was taken as reference (*11*). For supported samples, the Si 2*p* and O 1*s* lines were also used as references, and gave results not differing more than a few tenths of an eV from those obtained with the carbon reference. Since supported hexavalent chromium is reduced under the action of X-rays inside the spectrometer, the Cr peak was always recorded immediately after the sample had been introduced into the spectrometer. This was done to minimize the reduction and to have the same effect on all samples.

Reflectance Spectra

Optical reflectance spectra were recorded on a Beckman DK1 instrument, in the range 2500 nm to 210 nm at room temperature, with MgO as reference.

X-Ray Analysis

Diffraction patterns were obtained with Cu$K\alpha$ radiation, using a 114-mm diameter camera (Straumanis mounting). The observed lines were generally weak, not extending beyond $2\theta \sim 70°$. In order to improve the reliability of the measurement

of the reflection position more than one reading was carried out. A visual measuring devise capable of reading to 0.05 mm was used. The reproducibility was very satisfactory even on weak reflections.

The crystallite size determination has been carried out by diffractometric profile recording, with the procedure illustrated by Klug and Alexander (*12*). The instrumental broadening b was determined by recording a line at $2\theta = 36.6°$, arising from quartz (particles 8 to 12 μm), which was partially resolved for the α_1–α_2 doublet. A b value of 0.12° was obtained. The Cr_2O_3 line was at $2\theta = 33.6°$ and it was unresolved. From the observed breadth B_0 a value corrected for the α_1–α_2 doublet was obtained. The breadth due to crystallite size, β, was therefore obtained. A value of $K = 1$ in the Scherrer formula was adopted, and curve B of Fig. 9–5 of Ref. (*12*) was chosen (intermediate-shape profiles). A value of B_0 between 0.25 and 0.27° was generally observed, and the derived values of β were 0.14 to 0.18° depending on the specimen and on which curve, (a) or (b) of Fig. 9–4, Ref. (*12*), was adopted.

EXPERIMENTAL RESULTS

(a) *XPS of Pure Compounds*

Some XPS measurements were made on pure chromium compounds to obtain binding energy (BE) values (Table 1) for comparison with supported samples. The $2p$ peak is the most intense in the XPS spectrum of chromium and all considerations will be made on this peak, especially on supported samples, although the $3p$ peak shows a larger chemical shift (4 vs 3 eV) than the $2p^{\frac{1}{2}}$ peak in the change of oxidation state from Cr(VI) to Cr(III).

Several types of Cr_2O_3 sample were examined and their BE values were as follows: commercial products (575.7 eV), commercial products calcined at temperatures from 400 to 700°C (575.4 eV), specimens obtained by thermal decomposition of ammonium dichromate (575.5 eV), and a single crystal (575.6 eV). The average value, coincident with that obtained from the single crystal, is adopted for Cr_2O_3.

CrO_2 shows the same BE as Cr_2O_3, but the FWHM (full width at half maximum) is larger; this may indicate the presence of some Cr in more than one oxidation state, although X-ray diffraction revealed no impurity. The peaks of CrO_2 are displaced without any deformation, by an applied voltage, thus indicating that we have a conductor. The Cr $3s$ level shows a multiplet splitting of ~3.8 eV, the literature value for Cr_2O_3 being 4.1 eV (*13*).

The last column of Table 1 gives the intensity ratio of the components of the $2p$ doublet (area ratios). The theoretical value of this ratio is 2.

Data similar to those of Table 1 have already been reported in the literature (*13–17*), with the exception of those con-

TABLE 1

Sample	Cr $2p^{\frac{3}{2}}$	Cr $2p^{\frac{1}{2}}$	Cr $2p^{\frac{1}{2}}$–Cr $2p^{\frac{3}{2}}$	O 1s	$I^{\frac{3}{2}}:I^{\frac{1}{2}}$[b]
Cr_2O_3	575.6 (3.0)[a]	585.2	9.6	529.3 (1.8)[a]	1.85
$MgCr_2O_4$	575.6 (3.0)	585.4	9.8	529.2 (1.9)[a]	1.95
CrO_2	575.6 (3.9)	585.2	9.6	Peak rather broad, clearly composite	2.00
CrO_3	578.7 (1.6)	587.7	9.0	529.6 (2.3)	2.62
K_2CrO_4	578.4 (1.5)	587.4	9.0	529.0 (1.7)	2.73
$K_2Cr_2O_7$	578.7 (1.5)	587.9	9.2	529.2 (1.7)	2.55

[a] Full width at half maximum (FWHM) of the peak.
[b] Ratio of the peak areas of the components of the $2p$ doublet.

cerning $MgCr_2O_4$ and CrO_2. The different spin-orbit splitting and intensity ratio in hexavalent and trivalent chromium, as well as the larger chemical shift for the $3p$ as compared to the $2p$ levels, were reported by Helmer (*14*).

We found little difference in the BE of K_2CrO_7, K_2CrO_4, and CrO_3. Allen *et al.* (*15*) found a lower value of ~1 eV for CrO_3, while Morris and Westwood (*16*) reported a higher value for dichromate, so that the difference between K_2CrO_7 and CrO_3 was 4.1 eV. Connor *et al.* (*17*) reported values for Li_2CrO_4 and Na_2CrO_4 differing by 1 eV. Also, our FWHM's for the oxygen 1*s* and Cr $2p^{\frac{3}{2}}$ peaks are smaller than those of Allen *et al.* (*15*).

The higher FWHM of oxygen for CrO_3 in Table 1 may be due to the presence of the oxygen of adsorbed water, since this compound is hygroscopic. Some of these discrepancies in the BE values are likely to be due to the reference level used, while others are due to experimental and instrumental factors which are not always easy to control.

(*b*) *Supported Samples*

XPS measurements. Figure 1 reports the $2p^{\frac{3}{2}}$ peak of Cr for the sample CrSi 9 calcined at different temperatures. Figure 1 was obtained by drawing on transparent paper over the actual spectrum. One can notice the displacement of the intensity toward low BE as the temperature of treatment increases. The spectra can be explained as the sum of Cr(VI) and Cr(III). Cr(V) and Cr(IV) cannot be detected, owing to the width of the $2p^{\frac{3}{2}}$ peak, although small quantities of them may be present. Figure 1d illustrates the kind of curve decomposition that allows the estimation of the intensities of Cr(VI) and Cr(III) reported in Table 2. It is assumed that the relative sensitivities of Cr(VI) and Cr(III) are equal. Curve b and b′ of Fig. 1 report the spectrum of the same specimen recorded just after the introduction into the spectrometer (recording time 10 min) and after 30-min interval. The reducing effect of the X-ray beam is apparent. The spectra of the CrSi 1 sample showed very weak peaks, barely above the noise level, and did not allow the estimation of the relative amounts of Cr(VI) and Cr(III).

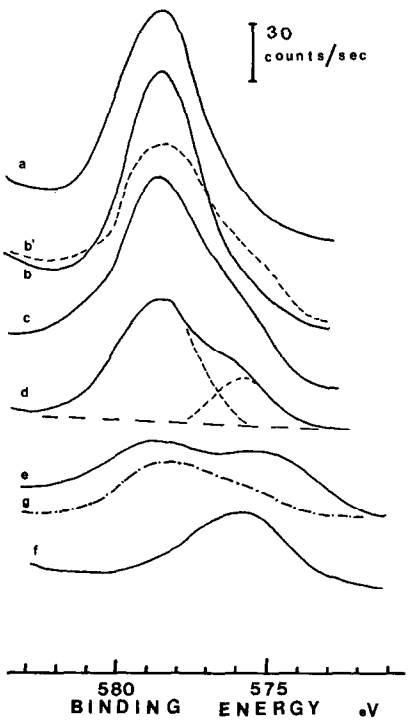

FIG. 1. XPS of the Cr $2p^{\frac{3}{2}}$ peak of the CrSi 9 sample, heated at different temperatures. Curve a: 120°C; curve b: 300°C; curve c: 350°C; curve d: 370°C; curve e: 400°C; curve f: 500°C. Curve b′ shows the spectrum of the same sample as curve b recorded 30 min after the sample was introduced into the spectrometer. Curve g refers to the CrSi 3 sample calcined at 435°C.

In the more intense spectra ($T < 400$°C) the signal to noise ratio was in the range 10 to 20. For the weaker spectra it was considerably lower (~3–4). This signal to noise ratio was the result of a compromise with the speed of recording. Longer recording times allow better signal to noise ratios but the instability toward reduction under X-ray irradiation made it imperative to record the spectra in the shortest time

TABLE 2

Sample	Temperature of treatment (°C)	X-ray	Reflectance	XPS, ratio Cr(VI):Cr(III)
CrSi 9	300	a	Cr(VI), P	10:0
	325	—	—	9:1
	350	β , γ, Cr_2O_3	Cr(VI), P	8.5:1.5
	370	(β), γ, Cr_2O_3	Cr(VI), Cr(III), P, B	8.5:1.5
	400	Cr_2O_3	Cr(VI), Cr(III), B	5:5
	500	Cr_2O_3	—	1:9
	700	Cr_2O_3	Cr(III), B	1:9
CrSi 5	300	a	Cr(VI)	10:0
	350	a	Cr(VI)	9:1
	380	CrO_2, Cr_2O_3	Cr(VI), B	9:1
	400	CrO_2, Cr_2O_3	Cr(VI), Cr(III), B	8:2
	450	Cr_2O_3	Cr(VI), Cr(III), B	5:5
	500	Cr_2O_3	—	4:6
	600	Cr_2O_3	—	4:6
	700	Cr_2O_3	Cr(III)	?
CrSi 3	365	a	Cr(VI)	10:0
	390	a	Cr(VI)	10:0
	410	a	Cr(VI)	10:0
	435	Cr_2O_3	Cr(VI), Cr(III), B	7.5:2.5
	465	Cr_2O_3	—	?
	490	—	Cr(VI), Cr(III), B	6:4
	600	—	Cr(VI), Cr(III), B	5:5
	700	—	—	5:5
CrSi 1	400	—	Cr(VI)	?
	500	a	Cr(VI)	—
	600	Cr_2O_3	Cr(VI), Cr(III)	?
	700	Cr_2O_3	Cr(VI), Cr(III)	?

Note: a = amorphous; P = peak at 800 nm; B = broad absorption in the 800–2500 nm region; ? indicates that the poor quality of the spectrum does not allow an estimate to be made.

possible. The X-ray induced reduction, however, could not be completely eliminated and introduced an error, which we estimate to be of the order of 5%, in the determination of the peak areas of Cr(VI) and Cr(III).

By taking the total (Cr(VI) + Cr(III)) intensity (area) of the $2p^{\frac{3}{2}}$ peaks of the four samples and plotting it against the temperature of treatment, Fig. 2 is obtained. The intensities are in arbitrary units and normalized to the Si 2*p* peak taken as equal to 200. Some points for the CrSi 1 sample are reported; although the spectra were very weak, a rough estimate of the total area could be made.

The most prominent feature of Fig. 2 is the drop of intensity in the 350–450°C region, indicating the formation of Cr_2O_3 crystallites much larger than the 10–20 Å of escape depth of the photoelectrons.

Reduction of a CrSi 5 sample at 500°C, in a stream of H_2, produced only a small decrease in the total intensity. Also, the X-ray induced reduction after several hours of exposure mentioned above, does not influence the total intensity as much as the high temperature treatment. This means

that agglomeration of Cr_2O_3 is strongly dependent on the conditions in which the heat treatment is carried out. Water vapor favors the growth of the Cr_2O_3 crystallites (*6*). The higher temperature at which the intensity of the samples drops, as the Cr concentration decreases, is an indication of the stabilizing influence of the support at lower Cr concentration.

XPS shows that the dispersed Cr_2O_3 obtained by heating CrSi9 in vacuum at 300°C can be almost completely reoxidized by heating at 300°C in air. The ease of reoxidation of dispersed CrO_3 has been previously demonstrated by using different techniques (*3*).

The initial intensities in Fig. 2, at 120°C, when only Cr(VI) is present, are not proportional to the amount of Cr present in the different samples. This is due to the fact that by increasing the Cr content the degree of dispersion decreases, so that a certain degree of clustering is present even before heat treatment in samples of higher Cr content.

X-ray analysis. The results of phase identification by X-ray analysis are summarized in Table 2. It can be observed that starting from the amorphous structure, each specimen changes with the temperature treatment towards a state showing the Cr_2O_3 lines. Before reaching this ultimate pattern, the more concentrated specimens CrSi 5 and CrSi 9 show complex patterns due to the contemporaneous presence of more than one phase, in particular the intermediate chromium oxide phases variously designated, of approximate composition Cr_3O_8 (hereafter called β), Cr_2O_5 (hereafter called γ) (*18–20*), and the CrO_2 oxide. While a study of their thermal stability is outside the scope of this work, the general sequence observed by previous investigators is maintained, but with some apparent displacement to higher temperatures for the β phase, as compared to earlier observations.

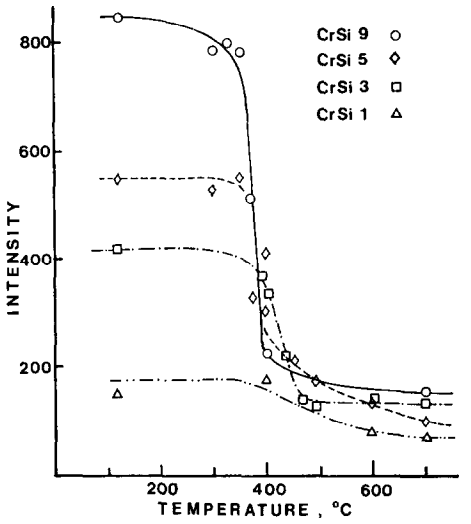

FIG. 2. Total intensity (CrVI + CrIII), in arbitrary units, of the $2p^{\frac{3}{2}}$ peak of Cr versus the temperature of heating for the four CrO_x/SiO_2 samples. The intensities are normalized to that of the Si $2p^{\frac{1}{2}}$ peak.

It can also be observed that the presence of Cr_2O_3, eventually observed even in CrSi 1 and CrSi 3, is detected at lower temperatures in the high chromium content samples. This fact might be due either to a displacement of the decomposition temperature (due to the interaction with the support) or to insufficient sensitivity towards the initial formation of Cr_2O_3 because of their particle size and/or limitation in quantity.

The crystallite size of Cr_2O_3 was measured for CrSi 9 heated at 370, 400, 700°C, and for CrSi 5 heated at 400°C, and the values thereby determined did not vary much, being around 600 Å. In view of the errors inherent with the procedure (*12*), a value of 400 Å is a limit for the smallest size compatible with the observed breadths. Smaller particles cannot be present in an amount which could give an appreciable contribution, unless their size is too small to give a diffraction pattern.

Diffuse reflectance measurements. The results of diffuse reflectance measurements are summarized in Table 2. The reflectance spectra of the CrSi 9 samples are reported

in Fig. 3. The spectra show two bands in the charge transfer region (278 and 370 nm) and the two *d–d* bands of Cr^{3+} in octahedral coordination ($A_{2g} \rightarrow T_{1g}$ at 463 nm, $A_{2g} \rightarrow T_{2g}$ at 600 nm).

Two other features, besides the H_2O bands in the 1200–1500 nm region, are worth noting in the spectrum of CrSi 9 (Fig. 3): these are a peak at 800 nm and a broad absorption centered around 1400 nm but covering most of the range 700–2500 nm.

The 800-nm peak is present only in the CrSi 9 sample, while the broad absorption can be seen also in other samples, though less pronounced. The 800-nm peak is present between 300 and 400°C, a temperature region where the intermediate phases β and γ are seen by X-rays (see Table 2). The peak is likely to be due to intermediate oxides, maybe with Cr in the oxidation states Cr(V) or Cr(IV). The broad band can also be attributed to intermediate phases, which are likely to be highly defective and conducting. The increasing absorption near 2500 nm, which is remarkable especially in the CrSi 5 sample, is probably due to conduction electrons, since some of the products formed during the decomposition of CrO_3 are good conductors, like CrO_2, whose presence is seen on CrSi 5 by X-ray diffraction (Table 2).

The spectra of samples at decreasing Cr concentration show the diminution of Cr(VI) and the appearance of Cr(III) as the temperature of heat treatment increases. The lower the Cr concentration, the higher the temperature at which Cr(III) appears. The stabilizing influence of the support on the higher oxidation states at lower Cr concentration is apparent. The band centered at 1400 nm is also strongly decreased.

Chemical analysis. Figure 4 reports the Cr(VI)/Cr(total) ratio for different specimens as a function of temperature. The trend previously observed by Deren and Haber (*3*) is confirmed. The resistance towards reduction is very marked for the dilute specimens. It should also be noticed that appreciable reduction takes place before the X-ray pattern shows any lines.

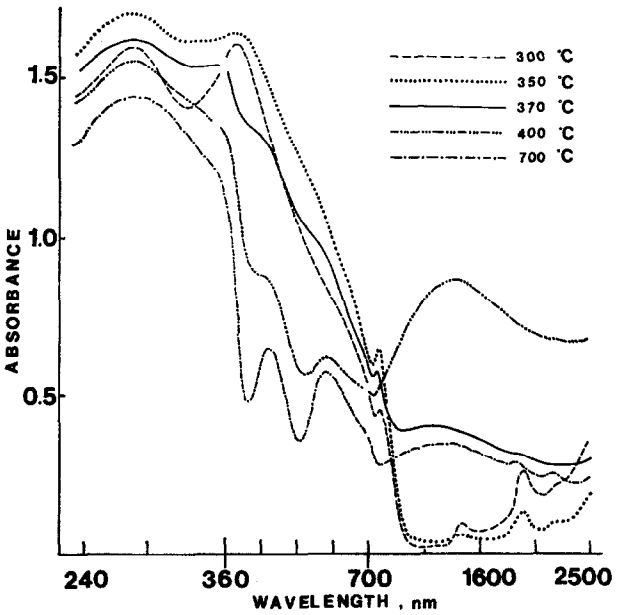

FIG. 3. Diffuse reflectance spectrum of the CrSi 9 sample heated at different temperatures.

At about 30% reduction (CrSi 9, 300°C; CrSi 5, 350°C) the amount of Cr_2O_3 formed should be visible, unless highly dispersed. Growth of Cr_2O_3 particles occurs very rapidly within a small temperature range, as can be deduced from the combination of chemical analyses and X-ray data of Table 2, and also reported at the bottom of Fig. 4.

DISCUSSION

Before considering in more detail the information that can be extracted from the data, particularly the XPS data, it is necessary to mention the fact that the XPS technique has a probing depth of about 10–20 Å. The escape depth, or mean free path, of photoelectrons in solids has been discussed by several authors (*21–23*). While no data are reported for Cr_2O_3, the choice of the 10–20 Å range is made on the basis of the reasonable assumption that the escape depth in chromium oxide is not too different from that in other oxides and metals. Compared to XPS, diffuse reflectance and X-ray diffraction are to be considered "bulk" techniques, their probing depth being one or more orders of magnitude larger.

The gradual reduction of Cr(VI) to Cr(III) as a function of temperature has been monitored with different techniques and it is interesting to compare the results, not only to stress the different features of each technique but also with the aim of drawing a picture of the textural aspects of the CrO_x/SiO_2 system.

Among the techniques used to study the dispersion of chromium oxide one can mention ESR, by which Derouane *et al.* (*24*) have recently shown that at temperatures above 350°C clustering occurs, a result confirmed by some of our data.

The Cr(VI):Cr(III) intensity ratio obtained in XPS measurements does not reflect the true ratio of the concentrations because Cr(VI) is dispersed on the surface mainly as a monolayer, chromate or dichromate-like (*6*), while Cr(III) forms the crystalline Cr_2O_3 phase, whose particle size is in the range of several hundred angstroms, as can be inferred from the X-ray diffraction data.

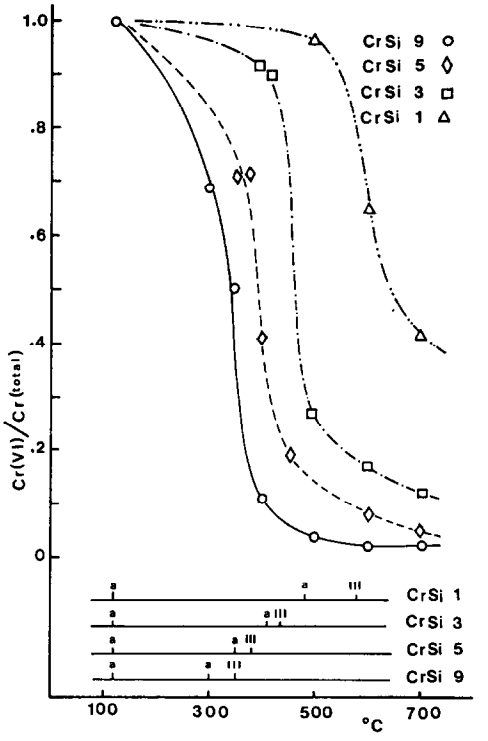

FIG. 4. The Cr(VI)/Cr(total) ratio versus the heating temperature, as determined by chemical analysis. At the bottom of the figure, the temperature at which Cr_2O_3 is revealed by X-ray diffraction is indicated. *a* Stands for amorphous; III stands for Cr(III).

Therefore, XPS, owing to the limited probing depth, can see most of the CrO_3, but only a fraction of the Cr_2O_3. This is the main reason for the fact that the Cr(VI):Cr(III) ratios obtained from chemical analysis are smaller than those given by XPS. The inability to see a substantial portion of chromium also explains the drop of the intensity in Fig. 2.

To explain the discrepancy in the Cr(VI):Cr(III) data, one can consider a simple model of the CrO_x/SiO_2 surface. While Cr(VI) tends to be molecularly dis-

persed, Cr(III) is present as Cr_2O_3 crystallites.

Let us assume that these crystallites are cubes of edge L (an assumption that does not greatly affect the results of our considerations). If d is the XPS probing depth, r the measured ratio of the peak areas Cr(VI):Cr(III), N^{VI} and N^{III} the total number of hexavalent and trivalent Cr species, and the suffix "seen" means the fraction seen by XPS, it can be shown that $N_{seen}{}^{III}/N^{III} = d/L$. The dispersion of CrO_3 allows one to put $N_{seen}{}^{VI} \sim N^{VI}$ with fair approximation and the following relationships hold:

$$N^{VI}/N^{III} = \frac{d}{L} r, \qquad N^{VI} + N^{III} = N$$

and

$$\frac{N^{VI}}{N} = \frac{rd}{rd + L}.$$

Let us consider the $N^{VI}:N^{III}$ ratio. The XPS values of this ratio are four to eight times larger than those found by chemical analysis. These differences cannot be explained by the factor d/L because, since $d = 20$ Å, L should have values in the 60 to 160 Å range. Such values of L would cause an excessive line broadening in the X-ray pattern, which is not found experimentally. A value of a few hundred angstroms for L, which is what one can infer from X-ray patterns, is in contrast with the observed N^{VI}/N^{III} ratio, since it would require much less Cr(VI) than actually found. It should be noted that variation of the d value does not alter the picture to a large extent since the discrepancy is of more than one order of magnitude. One is led to conclude that the "one-size" particle model does not hold. It would indeed be reasonable to think in terms of a size distribution of Cr_2O_3. However, the distribution should be such as to have a limited fraction of particles in the range which cause X-ray line broadening, and should not be very narrow, otherwise the same difficulties of matching the $N^{VI}:N^{III}$ value with the r value would be found. One can therefore imagine that the distribution of Cr_2O_3 is centered around two sizes, one very small (below the limit causing visible X-ray line broadening) and one fairly large giving rise to fairly sharp X-ray lines. For the sake of simplicity we will treat this second model as being made up of a "two-size" particle size distribution, one with $L \sim d$ and one with $L \sim 400$ Å, which is the lowest value compatible with particle size determination.

Let us call X_s the fraction of Cr(III) in small particles ($L \sim d$), $1 - X_s$ will be the fraction in the large particles. Then,

$$\frac{N^{VI}}{N^{III}} \Big/ r = X_s + (1 - X_s)d/L, \quad (1)$$

and if we match the above equation with the observed $(N^{VI}/N^{III})/r$ ratio (equal to $\frac{1}{4}$ to $\frac{1}{8}$, as said), one derives $X_s = 8$ to 20%.

In summary, one has the following picture of the morphology of Cr_2O_3: a fraction of it is present as small particles ($L \sim d$), while the remainder is present as particles of several hundred angstroms diameter that give a neat X-ray pattern. The broadening is not appreciable, most probably because the distribution of the L values is not uniform over the whole range of L. One can now inquire why the small Cr_2O_3 particles are formed. The texture of the small silica particles is not essentially affected by temperature treatments up to about 700°C. The silica particles do not a offer pores, but at the "neck" of each contact there is an area which defines a small volume. Chromium trioxide changing to Cr_2O_3 will interact more strongly with the support in these zones. Thus, while in the more open spaces the Cr_2O_3 formation is free to evolve towards large particles, in the "neck" zone small crystals are maintained. It should be noticed that even for the 1% chromium catalysts, where the

interaction with the support involves a large fraction of the total chromium after a high temperature treatment (though the temperature for the $CrO_3 \rightarrow Cr_2O_3$ transformation is shifted), the crystals of Cr_2O_3 are clearly visible with the X-ray technique, thus indicating the growth of Cr_2O_3. In the low-temperature treated material the reduction takes place before the X-ray technique can detect any Cr_2O_3. This type of reasoning shows that even for the low chromium content catalysts, after temperature treatment a fraction of Cr(III) must be present in small particles to match X-ray, chemical, and XPS data.

So far we have been concerned with the N^{VI}/N^{III} ratio. It is interesting to focus the attention on the value of the N^{VI}/N ratio, which is of course related to the former, taken at a temperature high enough for most of the chromium to be reduced to Cr_2O_3. From Eq. 1 one can now check that the N^{VI}/N ratio is in agreement with the observed chemical analysis (Fig. 4) for different r values, and for X_s values derived above. For CrSi 5 and CrSi 3, above 600°C (Table 2) we obtain for the two values of X_s given before ($X_s = 0.08$ to 0.20) the values $N^{VI}/N = 0.11$–0.21, while for CrSi 9 above 500°C we obtain $N^{VI}/N = 0.01$–0.02. These values are in good agreement with chemical data reported in Fig. 4. It can also be checked that varying the d/L value to 1/30 ($d \sim 20$ Å; $L = 600$ Å, as measured) does not appreciably affect the results.

Thus, XPS can be conveniently used for the characterization of supported oxide catalysts, together with the more traditional techniques. The capability of XPS to give information on the textural aspects of the supported oxide is particularly interesting.

ACKNOWLEDGMENT

We wish to thank Dr. M. Valigi for his assistance in the crystallite size determination.

REFERENCES

1. Clark, A., *Catal. Rev. 3*, 145 (1970).
2. Yermakov, Y., and Zakharov, V., *Advan. Catal.* **24**, 173 (1975).
3. Deren, J., and Haber, J., *Bull. Acad. Pol. Sci., Ser. Sci. Chim.* **12**, 663 (1964).
4. Matsumoto, A., Tanaka, H., and Goto, N., *Bull. Chem. Soc. Japan* **38**, 45 (1965).
5. Kazanskii, V. B., and Turkevich, J., *J. Catal.* **8**, 231 (1967).
6. Hogan, J. P., *J. Polymer Sci.* A-1 **8**, 2637 (1970).
7. Kazanskii, V. B., *Kin. Katal.* **11**, 455 (1970).
8. Zecchina, A., Garrone, E., Ghiotti, G., Morterra, C., and Borello, E., *J. Phys. Chem.* **79**, 966 (1975).
9. Groeneveld, C., Polymerization of ethene over chromium oxide–silica catalysts. Ph.D. Thesis, Technische Hogeschool, Eindhoven, 1974.
10. Deren, J., and Haber, J., Studies on the physicochemical and surface properties of chromium oxides. *Polska Acad. Nauk, Ceramika* **13**, 1 (1969).
11. Cimino, A., and De Angelis, B. A., *J. Catal.* **36**, 11 (1975).
12. Klug, H. P., and Alexander, L. E., "X-Ray Diffraction Procedures." J. Wiley, New York, 1962.
13. Carver, J. C., Carlson, T. A., Cain, L. C., and Schweitzer, G. K., *in* "Electron Spectroscopy" (D. A. Shirley, Ed.), p. 803. North-Holland, Amsterdam, 1972.
14. Helmer, J. C., *J. Electron Spectrosc.* **1**, 279 (1972).
15. Allen, G. C., Curtis, M. T., Hooper, A. J., and Tucker, P. M., *J. Chem. Soc., Dalton Trans.*, 1675 (1973).
16. Morris, A., and Westwood, N. P. C., *Inorg. Nucl. Chem. Lett.* **10**, 1009 (1974).
17. Connor, J. A., Hillier, I. H., Saunders, V. R., Wood, M. H., and Barber, M., *Molec. Phys.* **24**, 497 (1972).
18. Schwartz, R. S., Fankuchen, I., and Ward, R., *J. Amer. Chem. Soc.* **74**, 1676 (1952).
19. Glemser, O., Hauschild, U., and Trüpel, F., *Anorg. Allgem. Chem.* **277**, 113 (1954).
20. Kubota, B., *J. Amer. Ceram. Soc.* **44**, 239 (1961).
21. Klasson, M., Hedman, J., Berndtsson, A., Nilsson, R., Nordling, C., and Melnik, P., *Physica Scripta* **5**, 93 (1972).
22. Todd, C. J., and Heckingbottom, R., *Phys. Lett.* **42A**, 455 (1973).
23. Battye, F. L., Jenkin, J. G., Liesegang, J., and Leckey, R. C. G., *Phys. Rev.* **B9**, 2887 (1974).
24. Derouane, E. G., Hubin, R., and Mathieu, G., *Chem. Phys. Lett.* **33**, 571 (1975).